Homogeneous shear flow of a hard-sphere fluid: Analytic solutions

Janka Petravic*
Research School of Chemistry, The Australian National University, Canberra ACT 0200, Australia

Owen G. Jepps†
School of Science, Griffith University, Nathan, Brisbane Qld 4111, Australia

(Received 30 October 2002; published 13 February 2003)

Recently, a solution for collision-free trajectories in an N particle thermostatted hard-sphere system undergoing homogeneous shear (the so-called ''Sllod'' equations of motion) led to a kinetic theory of dilute hard-sphere gases under shear. However, a solution for collisions, necessary for a complete theory at higher densities, has been missing. We present an analytic solution to this problem, which provides surprising insights into the mechanical aspects of thermostatting a system in an external field. The equivalence of constant temperature and constant energy ensembles in the thermodynamic limit in equilibrium, the conditions for the nature of heat exchange with the environment (entropy creation and reduction) in the system, and the condition for appearance of the artificial string phase follow from our solution.

DOI: 10.1103/PhysRevE.67.021105 PACS number(s): 05.20.−y, 45.50.−j, 02.70.−c

I. INTRODUCTION

The nonequilibrium molecular dynamics algorithm for simulation of bulk Couette flow (the so-called ''Sllod'' algorithm) has been widely used in order to predict transport and structural properties of atomic and molecular fluids, both in the linear limit and in the non-Newtonian regimes. In principle, it provides a correct description of an isolated sheared system arbitrarily far from equilibrium [1].

This algorithm has been employed with a large variety of continuous effective potentials, providing insights into rheological properties of both simple and complex liquids. The hard-sphere limit is of interest because in a large number of simple liquids consisting of nearly spherical particles, the molecular motion is dominated by those portions of the intermolecular potential which are short ranged and harshly repulsive, while the longer-ranged interactions that have slow spatial variation play only a minor role. Hard spheres are also used to represent colloidal particles suspended in a fluid that then acts as an ideal homogeneous heat bath. In this case, the strain rates used in simulations approach the values that can be obtained in an experiment.

Let us consider a liquid placed between two plates parallel to the xy plane, where one of the plates moves in the x direction relative to the other with constant velocity. In the laminar regime, we expect the development of a linear streaming velocity profile. The streaming velocity $\mathbf{u}$ of a layer of fluid at a distance y from the reference plate is then equal to $\mathbf{i}\gamma y$, where $\mathbf{i}$ is the unit vector in the x direction, and $\gamma = \partial u_x / \partial y$ is the applied shear rate.

In this geometry, the Sllod equations of motion for the particles in the bulk fluid under shear are

$$\dot{\mathbf{r}}_i = \frac{\mathbf{p}_i}{m_i} + \mathbf{i}\gamma r_{yi}, \tag{1a}$$

$$\dot{\mathbf{p}}_i = \mathbf{F}_i - \mathbf{i}\gamma p_{yi}, \tag{1b}$$

where $\mathbf{r}_i$ and $\mathbf{p}_i$ are positions and momenta of particle i ($i = 1, \ldots, N$), with Cartesian components (r_{xi}, r_{yi}, r_{zi}) and (p_{xi}, p_{yi}, p_{zi}), respectively, and m_i are particle masses. For simplicity, we shall consider a two-dimensional system of hard disks of equal masses, $m_i = m$ for all particles i. Generalization to three dimensions is straightforward.

The total velocity of the particle i consists of the ''peculiar'' velocity $\mathbf{p}_i / m$ with the ''streaming velocity'' term $\mathbf{i}\gamma r_{yi}$ superimposed on it [Eq. (1a)]. The particles interact through conservative, pairwise additive forces $\mathbf{F}_{ij}$,

$$\mathbf{F}_i = \sum_{j \neq i}^{N} \mathbf{F}_{ij},$$

where $\mathbf{F}_{ij}$ is the force of particle j on particle i, and Newton's third law $\mathbf{F}_{ij} = -\mathbf{F}_{ji}$ is satisfied. The additional shear-dependent term in Eq. (1b) follows from the requirement that the system of equations (1) generate the correct expression for the dissipative flux [1].

The Eqs. (1) are used in simulation in conjunction with the ''sliding brick'' periodic boundary conditions [2] consistent with the shear rate γ in the equations of motion. The sliding-brick boundaries can alternatively be used with Newton's equations of motion, in order to create a ''boundary-driven'' shear flow with a linear streaming velocity profile within the simulation cell. The average behavior of the system is then equivalent to that obtained from the Sllod equations (1) [1]. The boundary-driven Lees-Edwards algorithm [2] was used in the pioneering nonequilibrium simulation of Naitoh and Ono [3] to compute shear-dependent viscosity of a hard-sphere fluid.

*Electronic address: janka@rsc.anu.edu.au
†Present address: Department of Chemical Engineering, University of Queensland, Brisbane Qld 4076, Australia. Electronic address: o.jepps@mailbox.uq.edu.au

The kinetic temperature T of the system is defined from the ''peculiar kinetic energy'' E_K and the equipartition theorem

$$\langle E_K \rangle = \left\langle \sum_{i=1}^{N} \frac{\mathrm{p}_i^2}{2m} \right\rangle = \frac{d}{2} N k_B T,$$

where d is the dimension of the system, k_B is the Boltzmann constant, and the angular brackets $\langle \cdots \rangle$ denote the ensemble average.

Shearing of a fluid produces viscous heating, which causes the peculiar kinetic energy and temperature to increase indefinitely over time. As a consequence, the system can never reach a well-defined steady state. The first method of temperature control was simple velocity rescaling. Naitoh and Ono [3] discarded it as unphysical, and used time scaling to calculate reduced properties as temperature increased.

Later, different continuous methods for removing adiabatic heating were proposed [1,4], which consisted of addition of a term of the form $-\alpha(\mathbf{r},\mathbf{p})\mathbf{p}_i$ to the right-hand side of Eq. (1b),

$$\dot{\mathbf{r}}_i = \frac{\mathbf{p}_i}{m_i} + \mathbf{i}\gamma r_{yi}, \tag{2}$$

$$\dot{\mathbf{p}}_i = \mathbf{F}_i - \mathbf{i}\gamma p_{yi} - \alpha \mathbf{p}_i .$$

The main problem with this type of thermostatting, in the case of a sheared fluid, is that it assumes that the streaming velocity profile created by Eqs. (1) is linear and equal to $\mathbf{i}\gamma r_{yi}$ for all shear rates. This is a good approximation of dissipative processes at low shear rates, but leads to unphysical suppression of velocity fluctuations and prevents the onset of turbulence at higher shear rates [5]. A remedy was found in the profile-unbiased thermostat [5] and recently, in a ''configurational temperature thermostat'' [7]. In this work, we present the analytic solution of the thermostatted Sllod equations (2) for hard spheres in the simplest case, where the thermostat multiplier α is determined using Gauss's principle of minimal constraint, so that both E_K and $K_0 \equiv E_K/m$ become constants of the motion, i.e.,

$$\alpha = \frac{1}{2K_0} \sum_{i=1}^{N} \mathbf{F}_i \cdot \mathbf{p}_i - \frac{\gamma}{2K_0} \sum_{i=1}^{N} p_{xi} p_{yi} . \tag{3}$$

One of our objectives is to determine, from the form of analytic solutions, what are the unphysical consequences of employing this thermostat, and in which circumstances they would have most impact.

In the hard-sphere limit, the interaction forces $\mathbf{F}_{ij}$ vanish during the free motion between the collisions, or are infinite during the infinitesimally short collision time. For a two-particle hard-sphere system under shear, the magnitude of the peculiar momenta is fixed by the isokinetic constraint [Eq. (3)], and Eqs. (2) can be reduced to the always-integrable one-body problem. In this case, both the free trajectories [6] and collisions [8,9] had been solved.

However, for $N>2$, the system of equations (2) has been considered impossible to solve for a long time because of the complexity introduced by the thermostat multiplier. Between collisions, when all $\mathbf{F}_i$ are zero, the motion of all particles is still coupled by the constraint given by Eq. (3). During a pair collision, when there is a nonzero force of interaction, only between the colliding pair, this force is present in all equations of motion via the thermostat multiplier. Recently, a solution of Eqs. (2) for free flight was found [10] by decoupling the force-free equations of motion between collisions. In what follows, we briefly review and discuss the free-flight solution and its implications, show how to solve the coupled collision equations, and discuss some physical implications of our solutions for the collisions.

II. FREE TRAJECTORIES

A. Solution

For hard disks of equal mass m between collisions, the system of equations (2) reduces to

$$\dot{r}_{xi} = \frac{p_{xi}}{m} + \gamma r_{yi}, \quad \dot{r}_{yi} = \frac{p_{yi}}{m}, \tag{4}$$

$$\dot{p}_{xi} = -\gamma p_{yi} - \alpha p_{xi}, \quad \dot{p}_{yi} = -\alpha p_{yi},$$

where the thermostat multiplier α has the form

$$\alpha = -\frac{\gamma}{2K_0} \sum_{i=1}^{N} p_{xi} p_{yi} . \tag{5}$$

All the momentum equations in Eqs. (4) are coupled via the thermostat multiplier, which satisfies a nonlinear second-order equation of motion,

$$\ddot{\alpha} + 6\dot{\alpha}\alpha + 4\alpha^3 = 0.$$

The general solution has the form

$$\alpha(t) = \frac{t - c_1}{c_2 - (t - c_1)^2}, \tag{6}$$

with the constants c_1 and c_2 determined from the initial conditions at $t=0$,

$$c_1 = \frac{\sum_i p_{xi}(0) p_{yi}(0)}{\gamma \sum_i p_{yi}(0)^2}, \quad c_2 = \frac{\sum_i \mathbf{p}_i(0) \cdot \mathbf{p}_i(0)}{\gamma^2 \sum_i p_{yi}(0)^2} - c_1^2. \tag{7}$$

There is no reference to the shear rate γ in the solution given by Eq. (6), all γ dependence is in the constants c_1 and c_2. The evolution of momenta and positions can now be obtained from Eq. (4) by direct integration,

$$p_{yi}(t) = p_{yi}(0) \sqrt{\frac{c_1^2 + c_2}{c_2 + (t - c_1)^2}},$$

$$p_{xi}(t)=[p_{xi}(0)-\gamma p_{yi}(0)t]\sqrt{\frac{c_1^2+c_2}{c_2+(t-c_1)^2}},$$

$$r_{yi}(t)=r_{yi}(0)+\frac{p_{yi}(0)}{m}\sqrt{c_1^2+c_2}\ln\frac{t-c_1+\sqrt{(t-c_1)^2+c_2}}{-c_1+\sqrt{c_1^2+c_2}},$$

$$\begin{aligned}r_{xi}(t)=&r_{xi}(0)+\gamma r_{yi}(0)t+2\frac{\gamma p_{yi}(0)}{m}\sqrt{c_1^2+c_2}[\sqrt{c_1^2+c_2}\\&-\sqrt{(t-c_1)^2+c_2}]\\&+\frac{p_{xi}(0)+\gamma p_{yi}(0)(t-2c_1)}{m}\sqrt{c_1^2+c_2}\\&\times\ln\frac{t-c_1+\sqrt{(t-c_1)^2+c_2}}{-c_1+\sqrt{c_1^2+c_2}}.\end{aligned}\tag{8}$$

In the equilibrium limit $\gamma=0$, the solutions in Eqs. (8) reduce to the familiar straight-line form,

$$\mathbf{p}_i(t)=\mathbf{p}_i(0),$$

$$\mathbf{r}_i(t)=\mathbf{r}_i(0)+\frac{\mathbf{p}_i(0)}{m}t.$$

In a hard-sphere system in equilibrium, change of temperature at constant density is equivalent to time scaling. From the form of solutions [Eqs. (8)] for thermostatted free trajectories under shear, we can see that in the same system (same m,σ,N), the same orbits in space would be followed by all particles at a constant ratio of $\gamma/\langle p\rangle=\gamma/T^{1/2}$. This means that increasing temperature at constant density is equivalent to time scaling of the same system with shear reduced by a factor of $T^{1/2}$.

The orbits and momenta of a three-particle system under shear are shown in Fig. 1. Particles move along curved trajectories, and their momenta rotate in the clockwise direction, approaching 0 if they were initially in the upper half plane and approaching $-\pi$ if they were initially in the lower half plane, their magnitudes changing as they move.

B. Discussion

From the form of the collision-free equations of motion [Eqs. (4) and (5)], one can deduce which trajectories contribute to viscous heating. The positive sign of the thermostat multiplier α corresponds to extraction of heat from the system, whereas negative α corresponds to a situation when heat is added to the system from the environment. Therefore, the trajectories that contribute to positive α in Eq. (5) are responsible for heat having to be extracted from the system, and the negative α are responsible for the need to add heat from the environment. In particular, when x- and y-momentum components have the same signs, i.e., when they are in the first and third quadrants and, therefore, oriented in the direction of change of streaming velocity along the direction of motion, heat needs to be added. The opposite

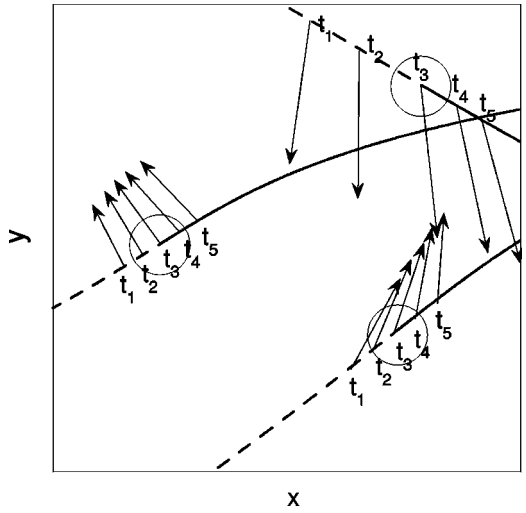

FIG. 1. Free trajectories of three hard disks and their successive momenta, according to Eq. (8), for the reduced number density of $\rho^*=N\sigma^2/L^2=3/64$, and the reduced shear rate $\gamma^*=m\gamma\sigma/(mk_BT^*)^{1/2}=0.455$.

orientation of momentum (second and fourth quadrants) results in heat having to be taken out. If motion is entirely in the x direction ($p_{yi}=0$), there is no change in peculiar kinetic energy even in an adiabatic process, and this particle does not contribute to the thermostat multiplier.

Another question that can be addressed is what would be the ''steady state'' of a sheared system without collisions. First, from the infinite time limit of the momentum evolution in Eqs. (7),

$$\lim_{t\to\infty}p_{xi}(t)=-\gamma p_{yi}(0)\sqrt{c_1^2+c_2},$$

$$\lim_{t\to\infty}p_{yi}(t)=0,$$

momenta of all particles tend to align along the $\pm x$ axis, with the infinite time limit of the thermostat multiplier equal to zero. During free motion under shear, momentum alignment is such as to minimize heat exchange with the environment. In this limit, there is no resistance to shear flow, and the steady state viscosity vanishes:

$$\eta_\infty=-\frac{1}{m\gamma V}\lim_{t\to\infty}\sum_{i=1}^{N}p_{xi}(t)p_{yi}(t)=0.$$

The hydrostatic pressure has only the kinetic component between collisions and is constant because of conservation of kinetic energy. However, the whole initial pressure

$$P(0)=\frac{1}{2}[P_{xx}(0)+P_{yy}(0)]=\frac{1}{2mV}\sum_{i=1}^{N}[p_{xi}^2(0)+p_{yi}^2(0)]$$

is in the infinite time limit all applied in the x direction,

$$\lim_{t\to\infty} P_{xx} = \frac{1}{mV} \lim_{t\to\infty} \sum_{i=1}^{N} p_{xi}^2(t)$$

$$= -\frac{\gamma^2}{mV}(c_1^2 + c_2) \sum_{i=1}^{N} p_{yi}^2(0) = P_{xx}(0) + P_{yy}(0),$$

$$\lim_{t\to\infty} P_{yy} = \frac{1}{mV} \lim_{t\to\infty} \sum_{i=1}^{N} p_{yi}^2(t) = 0.$$

However, collisions always occur, and the above collision-free limits are never reached [6].

III. COLLISIONS

A. Equations of motion for hard disks

Let us consider a system of N hard disks under shear, described by Eqs. (2) and (3), out of which disks numbered 1 and 2 are colliding. It is assumed that the force of interaction between 1 and 2 is central, purely repulsive, of constant (infinite) magnitude F throughout the distance σ, the diameter of the disk, and zero otherwise. In this case, the positions and momenta of the colliding particles obey the equations

$$\dot{r}_{x1,2} = \frac{p_{x1,2}}{m} + \gamma r_{y1,2}, \quad \dot{r}_{y1,2} = \frac{p_{y1,2}}{m},$$

$$\dot{p}_{x1,2} = \mp F_x - \gamma p_{y1,2} - \alpha p_{x1,2}, \quad \dot{p}_{y1,2} = \mp F_y - \alpha p_{y1,2}, \tag{9}$$

where $\mathbf{r}_{12} = \mathbf{r}_2 - \mathbf{r}_1$, $F_x = F(r_{x2} - r_{x1})/r_{12}$, $F_y = F(r_{y2} - r_{y1})/r_{12}$ are the Cartesian components of the force of interaction $\mathbf{F}$, and α is the Gauss thermostat multiplier. The thermostat multiplier, in general, given by Eq. (3), in this special case of only two colliding particles reduces to

$$\alpha = \frac{\mathbf{F}\cdot(\mathbf{p}_2 - \mathbf{p}_1)}{2K_0} - \frac{\gamma}{2K_0} \sum_{i=1}^{N} p_{xi} p_{yi}. \tag{10}$$

The equations of motion for other noncolliding particles $i > 2$ are

$$\dot{r}_{xi} = \frac{p_{xi}}{m} + \gamma r_{yi}, \quad \dot{r}_{yi} = \frac{p_{yi}}{m}, \tag{11}$$

$$\dot{p}_{xi} = -\gamma p_{yi} - \alpha p_{xi}, \quad \dot{p}_{yi} = -\alpha p_{yi}.$$

Note that the force of interaction between 1 and 2 figures in the equations of motion of all the particles because of the thermostat term.

In order to find the solution of the system of equations (9), (10), and (11) in the limiting case of hard disks, i.e., when $F \to \infty$, two points should be taken into account. First, as $F \to \infty$, all terms on the right-hand side of the momentum equations not containing F become negligibly small and can be neglected, so that

$$\dot{p}_{x1} = -F_x - \alpha p_{x1}, \quad \dot{p}_{y1} = -F_y - \alpha p_{y1}, \tag{12}$$

$$\dot{p}_{x2} = F_x - \alpha p_{x2}, \quad \dot{p}_{y2} = F_y - \alpha p_{y2},$$

$$\dot{p}_{xi} = -\alpha p_{xi}, \quad \dot{p}_{yi} = -\alpha p_{yi}, \quad i > 2,$$

where now

$$\alpha = \frac{\mathbf{F}\cdot(\mathbf{p}_2 - \mathbf{p}_1)}{2K_0}.$$

The strain rate γ does not appear in any of the Eqs. (12) in the infinite force limit. The terms containing the strain rate in the momentum equations are all finite and become negligible.

Second, in this limit, the duration of the collision τ, i.e., the time during which the particles interact becomes negligibly small, $\tau \to 0$. The total displacement of each of the particles is zero during the collision, and it is sufficient to solve only the momentum equations in the system (12).

The isokinetic system (12), unlike a system with conservation of total energy, does not in general conserve the momentum of the colliding pair,

$$\mathbf{p}_2 \neq \mathbf{p}_1.$$

Indeed, if the momenta of the particles 1 and 2 just before the collision are $\mathbf{p}_1$ and $\mathbf{p}_2$, and just after the collision are $\mathbf{p}_1'$ and $\mathbf{p}_2'$, so that

$$\mathbf{p}_1' = \mathbf{p}_1 + \Delta\mathbf{p}_1 \quad \text{and} \quad \mathbf{p}_2' = \mathbf{p}_2 + \Delta\mathbf{p}_2,$$

we cannot assume that $\Delta\mathbf{p}_1 + \Delta\mathbf{p}_2 = 0$. Only the momentum of the whole system is conserved.

The same is true of the kinetic energy. Since the infinite force appears in the momentum equations of all particles, all the momenta change during the collision. We cannot assume that the kinetic energy of the colliding pair is generally the same before and after the collision, and disregard the others. All particles take part in the collision even if they do not touch.

B. Solution

It is convenient to rewrite Eqs. (12) in terms of $\mathbf{p}_- = \mathbf{p}_2 - \mathbf{p}_1$ and $\mathbf{p}_+ = \mathbf{p}_2 + \mathbf{p}_1$ instead of $\mathbf{p}_1$ and $\mathbf{p}_2$, where

$$\dot{\mathbf{p}}_- = 2\mathbf{F} - \frac{\mathbf{F}\cdot\mathbf{p}_-}{2K_0}\mathbf{p}_-,$$

$$\dot{\mathbf{p}}_+ = -\frac{\mathbf{F}\cdot\mathbf{p}_-}{2K_0}\mathbf{p}_+.$$

The solution for $\mathbf{p}_-$ is the solution for the momentum of particle 2 in the ''relative'' reference frame in which particle 1 is stationary at the origin (Fig. 2).

Force $\mathbf{F}$ is central, i.e., directed along the vector $\mathbf{r}_{12}$. Therefore, we decompose the vector $\mathbf{p}_-$ into a ''radial'' component p_{r-} parallel to $\mathbf{r}_{12}$ and a ''tangential'' component p_{t-} perpendicular to $\mathbf{r}_{12}$,

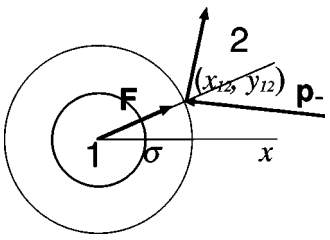

FIG. 2. The relative reference frame for colliding particles 1 and 2. Particle 1 is at rest, and the momentum of particle 2 is $\mathbf{p}_- = \mathbf{p}_2 - \mathbf{p}_1$, while its streaming velocity is γr_{y12}. Note that the angle of incidence is not necessarily equal to the angle of reflection, and that magnitudes of relative momentum before and after the collision do not have to be equal.

$$p_{r-} = \frac{\mathbf{p}_- \cdot \mathbf{r}_{12}}{r_{12}},$$

$$p_{t-} = \frac{-p_{x12} r_{y12} + p_{y12} r_{x12}}{r_{12}}.$$

With this decomposition, the thermostat multiplier becomes $\alpha = F p_{r-}/(2K_0)$, and the equations for p_{r-} and p_{t-} are

$$\dot{p}_{r-} = 2F\left[1 - \frac{p_{r-}}{4K_0}\right], \tag{13}$$

$$\dot{p}_{t-} = -F\frac{p_{r-} p_{t-}}{2K_0}. \tag{14}$$

The solution for the radial component is

$$p_{r-}(t) = \frac{p_{r-}(0) + 2\sqrt{K_0}\,\tanh(Ft/\sqrt{K_0})}{1 + [p_{r-}(0)/(2\sqrt{K_0})]\tanh(Ft/\sqrt{K_0})}, \tag{15}$$

and for the tangential component it is

$$p_{t-}(t) = \frac{p_{t-}(0)/\cosh(Ft/\sqrt{K_0})}{1 + [p_{r-}(0)/(2\sqrt{K_0})]\tanh(Ft/\sqrt{K_0})}. \tag{16}$$

In Eqs. (15) and (16), $p_{r-}(0)$ and $p_{t-}(0)$ are the radial and tangential components of relative momentum just before the collision. Note that Eqs. (15) and (16) are proportional to the pure hyperbolic tangent and hyperbolic cosine shifted in time so that at $t=0$, they are equal to $p_{r-}(0)$ and $p_{t-}(0)$, respectively. Therefore, the relative radial component is bounded between $-2K_0^{1/2}$ and $+2K_0^{1/2}$, and the tangential component has an extremum when the radial component vanishes [Fig. 3(a)].

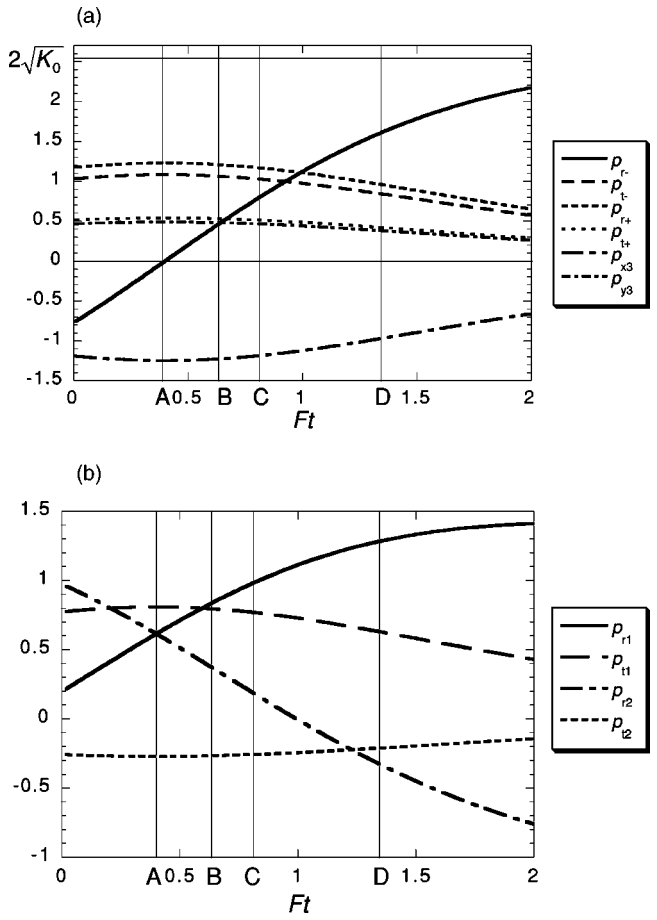

FIG. 3. Change of momenta during a collision of disks 1 and 2 in a three-hard-disk system. (a) Relative radial and tangential components according to Eqs. (15) and (16); (b) individual radial and tangential components of 1 and 2 according to Eqs. (17) and (18).

The equations for p_{r+} and p_{t+}, as well as for the Cartesian momentum components of the particles not taking part in the collision, have the same form as Eq. (14), with the solutions of the form Eq. (16). Solutions given by Eq. (16) are the momentum components just before the collision rescaled by the same factor.

Using Eqs. (15) and (16), we can find the radial and tangential momentum components of 1 and 2 in the laboratory frame just after the collision,

$$p_{r1,2} = \frac{p_{r+} \mp p_{r-}}{2} \quad \text{and} \quad p_{t1,2} = \frac{p_{t+} \mp p_{t-}}{2}.$$

Substitution yields the results

$$p_{r1,2} = \frac{1}{2}\,\frac{p_{r+}(0)/\cosh(Ft/\sqrt{K_0}) \pm p_{r-}(0) \pm 2\sqrt{K_0}\,\tanh(Ft/\sqrt{K_0})}{1 + [p_{r-}(0)/(2\sqrt{K_0})]\tanh(Ft/\sqrt{K_0})}, \tag{17}$$

$$p_{t1,2}=\frac{p_{t1,2}(0)/\cosh(Ft/\sqrt{K_0})}{1+[p_{r-}(0)/(2\sqrt{K_0})]\tanh(Ft/\sqrt{K_0})}, \qquad (18)$$

shown in Fig. 3(b). At the point $Ft=A$, the relative radial momentum of 1 and 2 p_{r-} vanishes [Fig. 3(a)], i.e., $p_1=p_2$ [Fig. 3(b)]. After $Ft=2A=C$, p_{r-} reverses sign, so that $p_{r-}(C)=-p_{r-}(0)$. This is a consequence of the parity of the hyperbolic tangent. At this point in time, the colliding particles exchange their radial momenta, while their tangential components, as well as the momenta of all the other particles, remain unchanged. The collision looks just like at constant total energy at zero shear. If the result is taken after a shorter time (point B) or after a longer time (point D), momentum and energy of the colliding pair are not conserved, and consequently the momenta of all other particles get rescaled.

By rearranging the expressions [Eqs. (15) and (16)], one can show that the kinetic energy of the whole system is conserved at all times,

$$\sum_{i=1}^{N} \mathrm{p}_i^2(t)=\sum_{i=1}^{N} \mathrm{p}_i^2(0)=2K_0.$$

Therefore, it is sufficient to solve Eqs. (13) and (14) and rescale all the other components by such a factor that the total kinetic energy is conserved.

If $p_{t1}=p_{t2}=0$ and $\mathbf{p}_i=0$ for $i>2$, the right hand side of Eq. (16) vanishes. In this pathological case of a ''head on'' collision of 1 and 2, with all other disks at rest, 1 and 2 pass through each other without a collision because their radial momenta are fixed by the thermostat. This is an isolated singularity of purely mathematical origin, which can be removed by interchanging $\mathbf{p}_1$ and $\mathbf{p}_2$ after the collision.

The solutions found so far describe the way in which momenta change during a hard-disk collision, but they do not determine when the collision stops and which are the final momentum values after the collision. In order to find this, we need to make use of the position equations.

C. End-of-collision condition in equilibrium

Let us look at the collision of particles 1 and 2 in more detail, in a reference frame where particle 1 is stationary at the origin, and is represented by a disk of radius σ, while particle 2 is represented by a point with momentum equal to (p_{r-},p_{t-}). The coordinates of the point 2 are $x_0=\sigma\cos\phi$ and $y_0=\sigma\sin\phi$ (Fig. 2).

During the collision, particle 2 moves infinitesimally towards the center of 1 (until it reaches the turning point), and after that, it moves away from the center until it is at a distance σ again. This is when the infinite force ceases to act, which defines the ''end of the collision.''

Since the particles are assumed to be spherical, the end-of-collision condition is that the total distance traveled by the ''point particle'' 2 in the radial direction during the collision is equal to zero.

In equilibrium, the radial velocity $\dot{r}$ of point 2 in this reference frame is equal to

$$\dot{r}(t)=|\dot{\mathbf{r}}_2(t)-\dot{\mathbf{r}}_1(t)|=\frac{p_{r-}(t)}{m}, \qquad (19)$$

so that the condition on the value of the quantity Ft at the end of collision is

$$\int_0^{\tau}\dot{r}(t)dt=\int_0^{\tau}\frac{p_{r-}(t)}{m}dt=0. \qquad (20)$$

The point at which the radial velocity given by Eq. (19) changes sign is the turning point [point $Ft=A$ in Fig. 3(a)]. The condition Eq. (20) can then be interpreted as a condition that the total area under the curve describing the evolution of $p_{r-}(t)$ from the start ($Ft=0$) to the end of the collision be equal to zero. From the symmetry of the hyperbolic tangent, it follows that the collision must then end at $Ft=2A=C$, twice the turning point time. As already mentioned, the radial momenta of the colliding particles are in this case exchanged, while their tangential components, as well as the momenta of other particles, remain unchanged. The ''collision rule'' at zero shear is the same for thermostatted and constant energy collisions, and the two systems cannot be distinguished from their trajectories at equilibrium.

D. End-of-collision under shear

The strain-rate dependent terms do not appear in the time-dependent solutions for the momenta in Eqs. (15) and (16). However, shear figures in the position equations (9) and Eqs. (11), changing the total velocities of all particles according to their positions. Therefore, the total radial velocity of the particle $\dot{r}$ in the relative reference frame is different from its equilibrium value, and depends on the polar angle ϕ of the collision as well as on the relative radial momentum p_{r-}. At the collision point (r_{x12},r_{y12}), the radial velocity is

$$\dot{r}(t)=\frac{p_{r-}(t)}{m}+\gamma\frac{r_{x12}r_{y12}}{\sigma}. \qquad (21)$$

The radial component of the streaming velocity $u_r=\gamma r_{x12}r_{y12}$ is constant during the collision because the position of particle 2 does not change in the infinite force limit. The end-of-collision condition which replaces Eq. (20) under shear, is

$$\int_0^{\tau}\dot{r}(t)dt=\int_0^{\tau}\left[\frac{p_{r-}(t)}{m}+\gamma\frac{r_{x12}r_{y12}}{\sigma}\right]dt=0. \qquad (22)$$

The sign of $u_r=\gamma r_{x12}r_{y12}$ depends on the quadrant where the collision occurs. If $r_{x12}r_{y12}<0$ (Fig. 4, shaded region), shear is ''pushing'' particle 2 towards particle 1, and the collision lasts longer than in equilibrium. On the other hand, if $r_{x12}r_{y12}>0$ (Fig. 4, white region), shear is pulling particle 2 away from particle 1, and the collision duration decreases.

The end-of-collision condition in the two cases is shown in Fig. 5. If $\mathbf{r}_{12}$ is directed along the change of the streaming velocity [inset in Fig. 5(a)], the magnitude of the relative radial momentum is reduced. If the alignment of the two disks is against shear [inset in Fig. 5(b)], then p_{r-} increases. As a consequence, when a collision occurs in the first or the

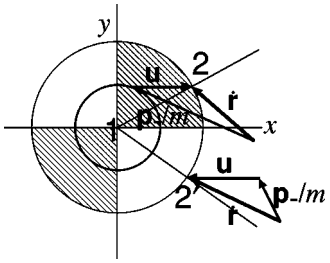

FIG. 4. Collision under shear according to Eq. (23) in the relative coordinate frame of Fig. 2. The full circle represents particle 1, the thinner circle is the scattering cross section. If the collision occurs in the first or in the third quadrant (white region), the radial component of the peculiar velocity is reduced by the radial component of the streaming velocity **u**. If the collision is in the second or fourth quadrant (shaded region), the total relative radial velocity is larger than p_{r-}/m. The vectors are defined in Eq. (21).

third quadrant, the angle of reflection is larger than the angle of incidence. In the case of a collision in the second or the fourth quadrant, particle 2 is deflected towards the line connecting their centers.

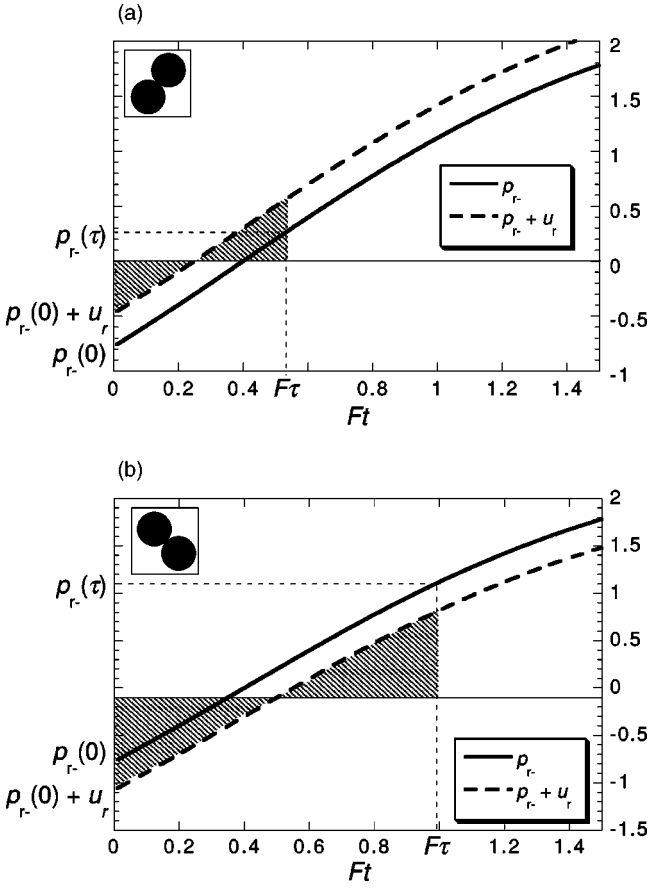

FIG. 5. End-of-collision condition under shear (a) when particle alignment is along shear, (b) when particle alignment is against shear. Full line: peculiar radial momentum. Dashed line: total radial momentum. The shaded region represents the end-of-collision condition under shear [Eq. (22)]: the area under the curve representing the integral of the total relative momentum $p_{r-}(Ft)+mu_r$ must vanish at the end of collision.

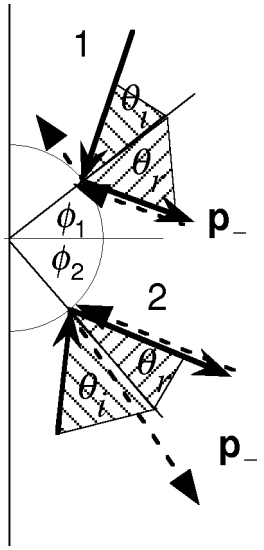

FIG. 6. Two types of collisions under shear. In case 1, the relative momentum $\mathbf{p}_-$ decreases and the angle of incidence θ_I is larger than the angle of reflection θ_R. In case 2, $\mathbf{p}_-$ increases and $\theta_I < \theta_R$. The dashed lines represent the relative momenta after time reversal.

In both cases, using some straightforward algebra, one finds for the end-of-collision time

$$\frac{F\tau}{\sqrt{K_0}} = \ln \frac{1-p_{r-}(0)/(2\sqrt{K_0})}{1+p_{r-}(0)/(2\sqrt{K_0})} + \ln \frac{1-mu_r/(2\sqrt{K_0})}{1+mu_r/(2\sqrt{K_0})}, \tag{23}$$

where the first term on the right hand side is the equilibrium collision time and the second term represents the interval by which the collision time is increased or reduced because of shear. The final value of $p_{r-}(\tau)$ is found by substituting Eq. (23) into Eq. (15).

Kratky and Hoover [11] used a method analogous to ours to solve the collisions of hard spheres in the Evans' algorithm for thermal conductivity [12]. However, in their case, there is no explicit streaming velocity term due to the field in the position equations of motion, so that the momentum and the kinetic energy of the colliding pair are conserved during the collision, and the motion of the other particles is unaffected.

E. Discussion

The two types of collision are shown in Fig. 6. The nature of heat exchange with the environment can be deduced from the behavior of the thermostat multiplier α during the collision. The total heat put into the system from the heat bath during a collision is

$$Q = \int_0^\tau \alpha(t)dt = \int_0^{\tau} \frac{Fp_{r-}(t)}{2K_0} dt = -\frac{m\gamma\sigma\cos\phi\sin\phi}{2K_0} F\tau. \tag{24}$$

The sign of Q depends only on the product $\cos\phi\sin\phi$. If the coordinates of the point of collision are in the first or in the

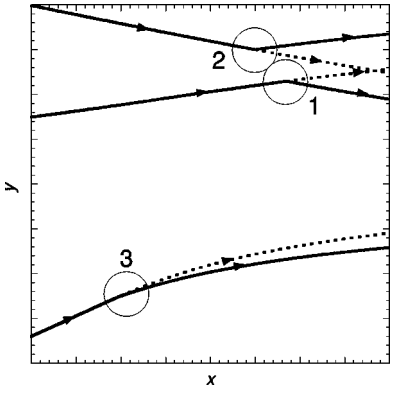

FIG. 7. Collision in a three-particle system under shear, reduced shear rate $\gamma^*=0.455$, reduced density $\rho^*=3/64$. Dashed lines would be the trajectories if there were no interaction (i.e., collision) between 1 and 2. Full lines are the trajectories with a collision. Disk 3 is deflected by the collision although it does not take part in it.

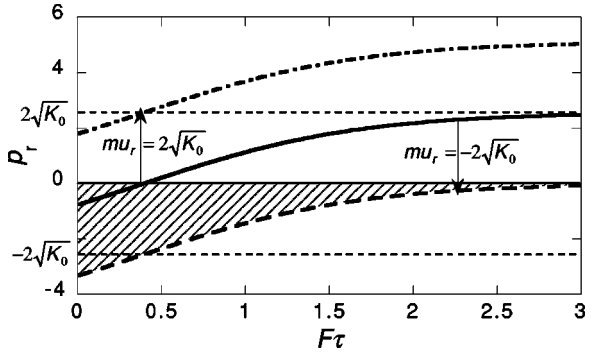

FIG. 8. When the relative radial streaming momentum $mu_r=m\gamma\sigma\cos\phi\sin\phi>2K_0^{1/2}$, there cannot be any collisions taking place at the point ϕ (dashed-dotted line) because the total relative radial momentum is always positive. When $m\gamma\sigma\cos\phi\sin\phi<-2K_0^{1/2}$, the colliding particles cannot pull apart after the collision (dashed line) because the shaded area cannot become positive [Eq. (25)].

third quadrant, the magnitude of the relative momentum $\mathbf{p}_-$ decreases and heat is added to the system ($Q>0$) in order to keep the temperature constant. This is case 1 in Fig. 6. On the other hand, for the collisions in the second or the fourth quadrant, the magnitude of $\mathbf{p}_-$ increases and heat needs to be taken out ($Q<0$). For the collisions at points $\phi=n\pi/2$, where n is an integer, or for $\gamma=0$, there is no heat exchange with the heat bath.

It is worth noting the fact that, if we reverse the momenta of all particles just after the collision, their trajectories would not retrace themselves. The same holds for the free trajectories. Indeed, the Sllod system of equations (2) is not time reversible, and the trajectories would reverse exactly only if each momentum and the strain rate γ all change sign. In this case, the conditions for the quadrants of the polar angle ϕ change as well.

Collisions of hard spheres contribute to heat exchange with the environment, otherwise all heat is generated during free motion between collisions.

When the magnitudes of momenta of the colliding particles change, the momenta of all the other particles get rescaled instantly in order to keep the total kinetic energy of the system constant. Therefore, all particles get deflected during a collision even though they have no direct interaction. This counterintuitive consequence of the solution for the sheared collision of hard spheres is always present, but the effect is more pronounced for smaller N. In Fig. 7, it is shown for a three-particle system.

F. Extreme shear

For a system of N hard disks at a given total kinetic energy $E_K=K_0/m$, the radial component of the relative momentum of a colliding pair p_{r-} must belong to the interval $[-2K_0^{1/2},2K_0^{1/2}]$. In order for a collision to occur, it is necessary for the total relative radial velocity $\dot{r}$ to be negative, i.e., for the particles to approach just before the collision.

Let $|u_r|=|\gamma\sigma\cos\phi\sin\phi|$ be the magnitude of the total relative radial velocity at some point on the circumference of a sphere of the diameter σ representing particle 1 in the relative coordinate system, as shown in Fig. 2. According to the collision rule given by Eq. (23) and shown in Fig. 5(a), this means that, for collisions in the first and third quadrants, particle 2 will collide with particle 1 only if $p_{r-}<-|mu_r|$. If the relative radial momentum p_{r-} is not negative enough, the collision will not occur, i.e., particle 2 will not even reach the point of collision.

Alternatively, from Fig. 5(b), collisions in the second and fourth quadrants can occur even if $p_{r-}>0$, if the condition $p_{r-}<|mu_r|$ is satisfied. Therefore, as strain rate increases, there is a higher probability of collisions occurring in the second and fourth quadrants, and a lower probability of collisions in the first and third quadrants.

The maximum value of $|\cos\phi\sin\phi|$ is equal to 1/2 when $\phi=\pm\pi/4$ or $\phi=\pm3\pi/4$, and the largest possible magnitude of the relative radial momentum of the colliding pair is $|p_{r-}|_{\max}=2K_0^{1/2}$. As a consequence, when

$$\gamma\geqslant\frac{4\sqrt{K_0}}{m\sigma}=\frac{2}{\sigma}\sqrt{\frac{2dNk_BT}{m}}, \tag{25}$$

there will be no collisions at points $\phi=\pi/4$ and $\phi=-3\pi/4$ (Fig. 8, dashed-dotted line). On the other hand, if a collision occurs at points $\phi=-\pi/4$ and $\phi=3\pi/4$, the total relative radial velocity at these points cannot become positive, and the two colliding particles can never go away from each other (Fig. 8, dashed line). If the strain rate increases further, such ''trapping'' collisions occur at increasing polar angle intervals $\Delta\phi$ around $-\pi/4$ and $3\pi/4$, whereas there are no collisions for $\phi=\pi/4\pm\Delta\phi$ and $\phi=-3\pi/4\pm\Delta\phi$.

This effect is related to the formation of the ''string phase'' observed in simulations of simple fluids with continuous potentials under strong shear [13]. In reality, if the system is large enough, the increase in shear rate invariably leads to turbulence [5]. Therefore, the string phase does not appear in bulk fluids under shear, unless turbulence is stabilized by some external force. In Gauss-thermostatted Sllod system of equations (2), such force is artificially provided by

the thermostat term, which strictly constrains the streaming velocity profile to be linear.

In a hard-sphere system, the string phase is a combination of trapping collisions and momentum alignment in free trajectories discussed in Sec. II B. The expression for the limiting shear rate in Eq. (25) suggests that the appearance of string phases in a Gauss-thermostatted system occurs at higher values of shear rate for larger system sizes, and that it would not occur in the thermodynamic limit. This is another indication of the artificial nature of the string phase in bulk sheared liquids.

IV. HYDROSTATIC PRESSURE AND SHEAR STRESS

The elements of the pressure tensor $P_{\alpha\beta}$ are given as the ensemble averages

$$P_{\alpha\beta}V=\left\langle \sum_{i=1}^{N}\frac{p_{\alpha i}p_{\beta i}}{m}\right\rangle+\left\langle \sum_{i=1}^{N-1}\sum_{j=i+1}^{N} r_{\alpha ij}F_{\beta ij}\right\rangle, \quad (26)$$

where α,β denote the Cartesian components x, y, and z, and V is the volume of the system. The first term on the right hand side represents the kinetic part and the second term is the potential part. The hydrostatic pressure P is defined as the trace of the pressure tensor divided by the dimension of the system,

$$P=\frac{1}{d}\sum_{\alpha=1}^{d} P_{\alpha\alpha}.$$

The pressure in Eq. (26) can be expressed as the time average,

$$P_{\alpha\beta}V=\lim_{t\to\infty}\frac{1}{t}\int_0^t\left(\sum_{i=1}^{N}\frac{p_{\alpha i}(s)p_{\beta i}(s)}{m}+\sum_{i=1}^{N-1}\sum_{j=i+1}^{N} r_{\alpha ij}(s)F_{\beta ij}(s)\right)ds.$$

In the case of hard spheres, free trajectories contribute to the kinetic part, whereas collisions contribute to the potential part. Let $\Delta t_1,\Delta t_2,\ldots,\Delta t_n$ be the times between $n+1$ collisions, so that $t=\Sigma\Delta t_i$. Let t_i be the time when the ith collision occurs, and τ_i the infinitesimal duration of the ith collision. Then the kinetic part of the pressure tensor is

$$P^K_{\alpha\beta}V=\lim_{t\to\infty}\frac{1}{t}\sum_n\int_{t_n}^{t_{n+1}}\sum_{i=1}^{N}\frac{p_{\alpha i}(s)p_{\beta i}(s)}{m}ds,$$

and the potential part is

$$P^P_{\alpha\beta}V=\lim_{t\to\infty}\frac{1}{t}\sum_n\int_{t_n}^{t_n+\tau_n} r_{\alpha 12}(s)F_{\beta 12}(s)ds=\lim_{t\to\infty}\frac{1}{t}\sum_n\frac{r_{\alpha 12}r_{\beta 12}}{\sigma}F\tau_n, \quad (27)$$

where $r_{\alpha 12}(t_n)$ are the relative coordinates of the nth collision point, and the product $F\tau_n$ in the limit $F\to\infty$ is determined from Eq. (23) for isokinetic collision under shear.

A. Kinetic part

The kinetic part of the hydrostatic pressure of hard spheres is

$$P^KV=\frac{1}{d}\sum_{i=1}^{N}\frac{p_i^2}{m}=\frac{2K_0}{dm}=Nk_BT,$$

the same constant value in equilibrium and in the Gauss-thermostatted sheared case. There can be no shear dilation in the kinetic part of the hard-sphere pressure.

The kinetic part of the shear stress is equal to

$$P^K_{xy}V=-\frac{K_0}{m\gamma V}\lim_{t\to\infty}\frac{1}{t}\sum_n\int_{t_n}^{t_{n+1}}\alpha(s)ds\approx-\frac{dNk_BT}{2\gamma V}\left\langle\frac{1}{\Delta t}\ln\frac{c_1^2-c_2}{(\Delta t-c_1)^2-c_2}\right\rangle,$$

where $\Delta t=\Delta t(c_1,c_2)$ is the mean time between collisions, and the angular brackets give an average over all possible initial conditions c_1 and c_2. This expression can be used in simulation to evaluate the kinetic contribution. It has been used to estimate the shear viscosity of an ideal gas using a self-consistent approach of kinetic theory [10].

B. Potential part

1. Equilibrium

From Eq. (27), the potential contribution to the hydrostatic pressure (the virial) for a two-dimensional system in equilibrium is

$$P^PV=\lim_{t\to\infty}\frac{\sigma}{2t}\sum_n F\tau_n=\frac{\sigma}{2}f_{\rm coll}\langle F\tau\rangle, \quad (28)$$

where $f_{\rm coll}$ is the collision frequency. In an isokinetic ensemble, the average transmitted impulse is

$$\langle F\tau\rangle_{NVT}=\sqrt{K_0}\left\langle\ln\frac{1-p_{r-}(0)/(2\sqrt{K_0})}{1+p_{r-}(0)/(2\sqrt{K_0})}\right\rangle, \quad (29)$$

where the average is taken over all possible values of p_{r-} just before the collision.

In the equilibrium constant energy ensemble, the product Ft can be shown [9] to be equal to

$$\langle F\tau\rangle_{NVE}=-2\langle p_{r-}(0)\rangle,$$

yielding a different hydrostatic pressure than for constant kinetic energy.

This result may seem paradoxical, given that from the outside, both systems look exactly the same — the same specular elastic collisions occur at the same time and trajectories follow the same rectilinear paths. However, in a ''soft''

repulsive potential, the two collisions would differ significantly. While in a constant energy system, the radial component would decrease till the turning point and increase in the opposite direction without any impact on the other momentum components of noncolliding particles, in the isokinetic collision, all momentum components of all particles change. In the latter case, with the same potential, the collision lasts longer and the two colliding bodies overlap more. The ratio of the two times remains different even in the hard-sphere limit.

The difference is the most obvious in the case of only two colliding hard disks. In the thermostatted system, the magnitudes of each of the two momenta are fixed to $\pm\mathbf{p}$ by the constant energy constraint. At any given point of collision, all possible orientations of the relative momentum (i.e., all values of the radial component between $-2p$ and 0) are then equally probable. The isokinetic and the constant energy virials then differ by a factor equal to half the Catalan constant, the isokinetic virial being nearly twice the constant energy virial [9].

For N disks, all possible orientations of the relative momentum are still equally probable, but not all magnitudes. From the central limit theorem, it follows that for large N, the probability of a disk having a momentum $\mathbf{p}$ is given by the Maxwell-Boltzmann distribution,

$$f(\mathbf{p})=\frac{\exp\{-\mathrm{p}^2/2mk_BT\}}{\int \exp\{-\mathrm{p}^2/2mk_BT\}d\mathbf{p}}.$$

It gives the probability of any relative momentum $\mathbf{p}_-$, and, in particular, that of the colliding particle 2, being equal to $\mathbf{p}$. The average impulse of Eq. (28) then becomes

$$\langle F\tau\rangle=\frac{\int_{\pi/2}^{3\pi/2}d\psi\int_0^{2\sqrt{K_0}}dp\ pF\tau(p,\psi)\exp\{-p^2/2mk_BT\}}{\pi\int_0^{2\sqrt{K_0}}dp\exp\{-p^2/2mk_BT\}},$$

where $\psi=\theta-\phi$ is the angle between $\mathbf{p}_-$ and $\mathbf{r}_{12}$.

In equilibrium, all initial orientations of relative momentum θ_i and all angles of impact ϕ (Fig. 6) that lead to a collision, i.e., such that $p_{r-}<0$, are equally probable. The radial component of the relative momentum in terms of angles θ_i and ϕ is $p_{r-}=p\cos(\theta-\phi)$, where p is the magnitude of the relative momentum $\mathbf{p}_-$, and the condition $p_{r-}<0$ means $\phi\in[0,2\pi]$ and $\psi=(\theta-\phi)\in[\pi/2,3\pi/2]$. The duration of a collision τ is a function of the magnitude of the relative momentum p and the angle ψ, $\tau=\tau(p,\psi)$. The form of $F\tau(p,\psi)$ for the isokinetic equilibrium collision is given by Eq. (23) for $u_r=0$.

Using Taylor expansion of the mean isokinetic collision impulse $\langle F\tau\rangle_{NVT}$ in terms of $p/(mNk_BT)^{1/2}$ as $N\to\infty$,

$$\lim_{N\to\infty}\langle F\tau\rangle_{NVT}=\lim_{N\to\infty}2\sqrt{mNk_BT}\ln\frac{1-p\cos\psi/(2\sqrt{mNk_BT})}{1+p\cos\psi/(2\sqrt{mNk_BT})}$$

$$=-\frac{p\cos\psi}{(mNk_BT)^{1/2}}-\frac{p^3\cos^3\psi}{12(mNk_BT)^{3/2}}+\cdots,$$

we find the ratio of isokinetic and constant energy pressures in two dimensions in the thermodynamic limit,

$$\lim_{N\to\infty}\frac{P^P_{NVT}}{P^P_{NVE}}=\lim_{N\to\infty}\frac{\langle F\tau\rangle_{NVT}}{\langle F\tau\rangle_{NVE}}\approx 1+\frac{1}{6N}+O\left(\frac{1}{N^2}\right).$$

The pressures in the two ensembles approach in the thermodynamic limit as $1/N$. The difference in pressures in the two ensembles, decreasing with the system size N, has been observed numerically in Ref. [11]. The $1/N$ approach of pressures is in accordance with the general proof of equivalence of equilibrium ensembles presented in Ref. [14].

2. Shear

In a thermostatted sheared system, the expression for the virial becomes

$$P^PV=\frac{\sigma}{2}f_{\mathrm{coll}}\frac{\int d\phi\int d\psi\int dppf(p,\phi,\psi)F\tau(p,\phi,\psi)}{\int d\phi\int d\psi\int dppf(p,\phi,\psi)}.$$

The magnitude of the peculiar momentum does not necessarily follow a distribution of Maxwell-Boltzmann type, but the deviations should be negligible in the thermodynamic limit and for small shear rates [1]. In the angular integration, however, the differences do not disappear in the thermodynamic limit because they are related to the change in the streaming velocity across the hard-disk diameter σ. The limits of integration for the angular variables are now such that the relative total radial velocity is negative,

$$\cos\psi\leqslant-\frac{m\gamma\sigma}{2p(0)}\sin 2\phi,$$

and the angular distributions are no longer uniform. Therefore, the first term on the right hand side of Eq. (23) changes its value, although its form is the same as in equilibrium. There is also an additional term to $F\tau$ [the second term on the right-hand side of Eq. (23)] with a nonvanishing γ-dependent leading term when $N\to\infty$. Taylor expansion of this term gives

$$\sqrt{K_0}\ln\frac{1-m\gamma\sigma\sin 2\phi/(2\sqrt{K_0})}{1+m\gamma\sigma\sin 2\phi/(2\sqrt{K_0})}\approx-\frac{m\gamma\sigma}{2}\sin 2\phi$$

$$-\frac{2}{3K_0}\left(\frac{m\gamma\sigma}{4}\right)\sin^3 2\phi+\cdots.$$

All the terms in the Taylor expansion would vanish for a uniform distribution of ϕ with the same limits as in equilib-

rium because they contain powers of $\sin 2\phi$. However, because of the change of limits and nonuniform angular distribution, the first term on the right hand side gives a finite contribution for all system sizes. The exact final form of the virial is a result of interplay between the change in the peculiar momentum distribution during free flight and collisional mapping, and can be deduced most easily by computer simulation.

The integrand of the shear stress expression is equal to the integrand for the hydrostatic pressure multiplied by an additional factor of $\sin 2\phi$. This causes it to vanish in equilibrium and become finite when $\gamma \neq 0$ even in the thermodynamic limit.

V. CONCLUSION

We have presented an analytic solution for collisions in a sheared hard-sphere liquid thermostatted using a Gauss isokinetic constraint.

Our solution shows that, in equilibrium, the hydrostatic pressures calculated in the constant energy and the constant temperature ensembles differ, although the trajectories in the two ensembles are indistinguishable. The difference is system-size dependent and disappears in the thermodynamic limit, with a leading term proportional to the inverse of the number of particles.

With these equations of motion, collisions under shear conserve neither the momentum nor the kinetic energy of a colliding pair, only the energy and the momentum of the system as a whole. As a consequence, the angle of reflection is not equal to the angle of incidence, and all trajectories are deflected after a collision, irrespective of whether the particles were actually colliding or not. Under extreme shear, the collision law predicts instability equivalent to the string phase appearing in strongly sheared continuous systems. This instability occurs at higher shear rates for larger system sizes, and would disappear in the thermodynamic limit.

Among the features of collisions in this system, their ''nonlocal'' character seems the most counterintuitive. However, the same unphysical nature of representing collisions under shear, as shown in Fig. 7, is shared by all continuous kinetic thermostats described in Ref. [4], because they rely on the coupling of all motion in order to define and conserve the temperature of the system. When such a method is used to control peculiar momenta with respect to a nonzero streaming velocity profile, it causes the change of direction of all trajectories in a finite system. This is not so obvious in systems with continuous interparticle interactions because there the collisions are not clearly defined and there are no discontinuous changes of momenta. On the other hand, this effect is significant only for strongly sheared small systems, and becomes infinitesimal in the thermodynamic limit. Therefore, the Gauss kinetic thermostat is still a good approximation of the process for large systems and low shear rates. For very high shear rates, the nonlocality of collisions would be visible even for large system sizes, but then an even more serious objection is the assumption of the linear streaming velocity profile in Eq. (3).

It is important to bear in mind that the objective of introducing an artificial thermostat in nonequilibrium molecular dynamics simulations is not to reproduce the microscopic details of heat transfer, but to account for its macroscopic effects. In doing so, we must choose which properties need to be retained in a particular model. Let us consider two of the most important applications of the hard-sphere model in computer simulations—granular matter and colloidal dispersions.

In simulations of granular matter, heat is extracted only in collisions through the coefficient of restitution. This reflects the fact that granular particles are macroscopic objects with many internal degrees of freedom, and ''heat transfer'' consists largely of loss of center-of-mass kinetic energy due to friction. In a colloidal suspension, on the other hand, the solvent acts as a ''heat bath'' for the dispersed solid particles, and is otherwise not present in a simulation. In this case, using our solutions in simulation of colloidal systems under shear provides an equally acceptable approximation for representing such a system by hard spheres in a void in the first place, provided that the shear rate is sufficiently small and the system is sufficiently large.

ACKNOWLEDGMENT

The authors would like to thank Professor William G. Hoover for helpful suggestions regarding this work.

[1] D.J. Evans and G.P. Morriss, *Statistical Mechanics of Nonequilibrium Liquids* (Academic Press, London, 1990).
[2] A.W. Lees and S.F. Edwards, J. Phys. C **5**, 1921 (1972).
[3] T. Naitoh and S. Ono, J. Chem. Phys. **70**, 4515 (1979).
[4] W.G. Hoover, K. Aoki, C.G. Hoover, and S.V. De Groot, Physica D (to be published).
[5] D.J. Evans and G.P. Morriss, Phys. Rev. Lett. **56**, 2172 (1986).
[6] A.J.C. Ladd and W.G. Hoover, J. Stat. Phys. **38**, 973 (1985).
[7] L. Lue, O.G. Jepps, J. Delhommelle, and D.J. Evans, Mol. Phys. **100**, 2387 (2002).
[8] J. Petravic, D.J. Isbister, and G.P. Morriss, J. Stat. Phys. **76**, 1045 (1994).
[9] J. Petravic and D.J. Isbister, Phys. Rev. E **51**, 4309 (1995).
[10] R. van Zon, Phys. Rev. E **60**, 4158 (1999).
[11] K.W. Kratky and W.G. Hoover, J. Stat. Phys. **48**, 873 (1987).
[12] D.J. Evans, Phys. Lett. **91A**, 457 (1982).
[13] J.J. Erpenbeck, Phys. Rev. Lett. **52**, 1333 (1984).
[14] D.J. Evans and S. Sarman, Phys. Rev. E **48**, 65 (1993).